Comparative analysis of genes downstream of the Hoxd cluster in developing digits and external genitalia

John Cobb and Denis Duboule*

National Research Center (NCCR) 'Frontiers in Genetics', Department of Zoology and Animal Biology, University of Geneva, Sciences III, Quai Ernest Ansermet 30, 1211 Geneva 4, Switzerland
*Author for correspondence (e-mail: denis.duboule@zoo.unige.ch)

Accepted 29 April 2005

Development 132, 3055-3067
Published by The Company of Biologists 2005
doi:10.1242/dev.01885

Summary

Mammalian Hox genes encode transcription factors that are crucial for proper morphogenesis along the various body axes. Despite their extensive structural and functional characterization, the nature of their target genes remains elusive. We have addressed this question by using DNA microarrays to screen for genes whose expression in developing distal forelimbs and genital eminences was significantly modified in the absence of the full Hoxd gene complement. This comparative approach not only identified specific candidate genes, but also allowed the examination of whether a similar Hox expression pattern in distinct tissues leads to the modulation of the same or different downstream genes. We report here a set of potential target genes, most of which were not previously known to play a role in the early stages of either limb or genital bud development. Interestingly, we find that the majority of these candidate genes are differentially expressed in both structures, although often at different times. This supports the idea that both appendices involve similar genetic controls, both upstream and downstream of the Hox gene family. These results highlight the surprising mechanistic relationship between these rather different body parts and suggest a common developmental strategy to build up the most distal appendicular structures of the body, i.e. the digits and the penis/clitoris.

Key words: Hox genes, Development, Penis, Clitoris, *Sgk*, *Epha3*, Mouse

Introduction

In the course of tetrapod development, both the limbs and the external genitalia first appear as small buds of mesenchymal cells. The mouse forelimb bud begins to emerge from the lateral plate mesoderm during the ninth day of embryonic development (E9) and the genital tubercle (genital bud; genital eminence) becomes visible at E11.0. The subsequent elongation of both structures is dependent on the epithelial-mesenchymal interactions that establish a signaling center at the distal end of the growing bud: the apical ectodermal ridge (AER) in limbs and the distal urethral epithelium (DUE) in the presumptive genitals. During outgrowth, the proliferating mesenchymal cells of the limb bud are patterned and differentiate into mature limb structures in a proximal to distal sequence (reviewed by Tickle, 2003). Although the patterning of the genitalia has not been studied as extensively, the time-dependent development of proximal and distal segments and the presence of a bony structure (os penis/baculum in males or os clitoris in females) in many mammalian genital organs suggests a common ontogenetic strategy. Therefore, despite the rather different fate of these two structures, their basic underlying morphogenetic processes are similar.

Over the past 15 years, gene expression analyses and functional approaches have largely substantiated the surprising similarity between the distal part of developing limbs (the digits) and the genitalia. Indeed, the majority of genes known to be of interest for developmental growth and patterning in presumptive digits are also transcribed in the emerging genital bud. The initial outgrowth of the limb bud is dependent on the production of retinoic acid by the enzyme ALDH1A2 (RALDH2) (Niederreither et al., 2002), whose expression also suggests a role in the formation of the genital bud. Fibroblast growth factor (FGF) signaling is required for both AER and DUE function (Haraguchi et al., 2000; Sun et al., 2002). In the limb, expression of the sonic hedgehog gene (*Shh*) from a posterior patch of mesodermal cells called the zone of polarizing activity (ZPA) is required for both anteroposterior and proximodistal patterning (Riddle et al., 1993). In developing genitals, *Shh* expression in the urethral epithelium, rather than the mesoderm, is required for outgrowth of the bud (Haraguchi et al., 2001; Perriton et al., 2002). The significance of these homologous expression patterns is confirmed by gene inactivation experiments, which often cause phenotypic effects in both structures (e.g. Dolle et al., 1993).

The patterning of the autopod domain of the limb, which corresponds to the hands and feet, is of particular interest in this context. For example, the expression patterns of the genes coding for the transcription factors of the HOX family are comparable in both the genitalia and in distal limbs (Dolle et al., 1991). Specifically, the Hoxa and Hoxd genes related to the *Drosophila Abd-B* gene, located at the 5′ extremity of their respective clusters, are necessary for patterning both the digits and genitalia. The most 5′ genes from each complex, *Hoxa13* and *Hoxd13*, are the ones that are most strongly expressed at

the distal ends of limbs and in the genital bud. The combined inactivation of *Hoxa13* and *Hoxd13* in the same animal leads to the agenesis of both external genitalia and distal limbs (Fromental-Ramain et al., 1996; Kondo et al., 1997). Analyses of compound *Hoxa13*/*Hoxd13* mutants revealed that effects of these null mutations are dose-dependent in genitals, in the digestive and urogenital tracts (Warot et al., 1997), and in limbs (Zakany et al., 1997). Likewise, a variety of human congenital syndromes involving mutations in either *HOXD13* or *HOXA13* are characterized by morphological defects in both digits and genitalia (Goodman, 2002).

These observations raise the question of how the same set of control genes, active in similar developmental processes, ultimately generates morphologically and functionally different structures. One possibility is that Hox transcription factors regulate the expression of different target genes depending on the ontogenetic context. Interestingly, there is little information about the identity of HOX-dependent target genes during limb patterning, and their relationships with either the FGF, WNT, SHH, BMP or retinoid signaling pathways are unclear. Recent studies have begun to address these questions. In one approach, candidate genes were chosen because of their known role in the patterning pathways outlined above. In this way Knosp et al. (Knosp et al., 2004) identified *Bmp2* and *Bmp7* as being downstream of *Hoxa13* in limb development, and a related study showed that *Bmp7* and *Fgf8* expression is dependent on *Hoxa13* in genitals as well (Morgan et al., 2003).

A more comprehensive method is to use microarray technology because in this case no prior knowledge of candidate genes is required. One approach is to express Hox genes in cell lines where they are normally not expressed, and then compare expression profiles with and without Hox expression. In this way, *Itga8* was established as a target of *Hoxa11* regulation in the developing kidney (Valerius et al., 2002). A perhaps more physiologically relevant method is to compare expression in tissues from wild-type and Hox-mutant mice. With such a technique, Hedlund et al. (Hedlund et al., 2004) identified candidate target genes by comparing embryonic spinal cord tissue from wild-type and *Hoxd10*-null mice. In a related approach, Pruett et al. (Pruett et al., 2004) used transgenic mice overexpressing the *Hoxc13* gene to identify keratin genes of the *Krtap16* family as likely direct targets of HOXC13. The use of such approaches is nevertheless complicated by the severity of some Hox mutations and the functional redundancy of these genes. If the mutation is severe enough to radically transform tissues, expression profiling would undoubtedly identify many candidate genes as, effectively, different structures would be being compared. However, the relevance of these candidates would be unclear, because in this case the genes immediately downstream would be difficult to differentiate from the many genes far downstream that are necessary to form the structure. Therefore, we chose not to use a mutant with a drastic phenotype such as the *Hoxa13*/*Hoxd13* double mutant described above. Using this or comparable strains would preclude a comparative approach as external genitalia and distal limbs do not develop in these mutants.

Instead, we analyzed a mutant with an intermediate phenotype in which the genitalia and distal limbs were partially, but not completely, lost. We used a mouse strain deleted for the entire Hoxd cluster ($HoxD^{Del1–13}$). When Hoxd genes are deleted, the digits and external genitalia are reduced in size, but the basic pattern of both structures, as well as the relative amount of cell types, apparently remains intact (Zakany and Duboule, 1996; Zakany et al., 1997). Because of the common expression patterns of Hoxd genes in genitals and digits, and the related phenotypic effects of their mutations, we hypothesized that genes downstream of Hoxd could be similarly regulated in both structures. Therefore, we simultaneously identified candidate genes in distal forelimbs and genitals by analyzing global gene expression in both tissues, in both the presence and absence of Hoxd genes. The advantage of this comparative strategy is that in addition to identifying specific candidate genes, we can also begin to characterize the general nature of gene expression programs downstream of the Hoxd genes in two distinct structures, and therefore address the effects on gene expression of an evolutionary-conserved Hox expression pattern.

Candidate genes were identified by microarray analysis and subsequently validated by complementary approaches: real-time RT-PCR and in situ hybridization. Only a minority of candidate genes identified in either tissue appeared to be Hoxd dependent in just one of the two structures. This suggests that expression of the same Hox genes in two different developmental contexts modulates at least a subset of overlapping downstream genes. Furthermore many of the identified genes were not previously known to have any role in limb or genital development, and most are not part of any of the established limb or genital patterning pathways.

Materials and methods

Mice and RNA samples

The $HoxD^{Del1–13}$ (previously called *Del9*) and $HoxD^{Del1–10}$ alleles have been previously described (Spitz et al., 2001; Zakany et al., 2004). *Hoxa13*-mutant mice were provided by P. Chambon and have been previously described (Fromental-Ramain et al., 1996). $HoxD^{Del1–13}$ heterozygous mice from a mixed C57BL/6-129/Sv background were crossed to give homozygous mutant and wild-type embryos. Noon on the day of plugging was assumed to be E0.5. For microarray analysis, E12.5 embryos were dissected by cutting the autopod of the forelimbs with fine forceps and by removing the genital bud with a tungsten needle. The precise point of cutting for each tissue is indicated by arrows in Fig. 1A. Samples were immediately placed in RNAlater reagent (QIAGEN) for storage during genotyping.

The RNA samples used for microarray analysis (herein referred to as primary samples) were extracted from pools of limb or genital tissue from five to 10 individual embryos of the same genotype, three replicate pools for each tissue and genotype. RNA was isolated using the RNeasy micro- or mini-kit (QIAGEN), following homogenization and disruption with a POLYTRON device (Kinematica) using the QIAGEN RLT solution. The yield of total RNA was 5-7 μg per pool of genital tissue and 20-45 μg per pool of limb tissue. The quality of all RNA pools was confirmed by analysis on a 2100 Bioanalyzer (Agilent). Secondary samples for quantitative real-time RT-PCR analysis were collected in triplicate from E11.5-E14.5 embryos and extracted as above, except that in most cases a sample from only one individual embryo was used per replicate.

Microarray analysis

Double-stranded cDNA was synthesized from 2-5 μg total RNA from each pool, according to the GeneChip Expression Analysis Technical Manual (Affymetrix), using the SuperScript Choice system (Invitrogen). cDNA was used to synthesize biotin-labeled cRNA using

the BioArray HighYield RNA Transcript Labeling Kit (Enzo). After purification using a QIAGEN RNeasy column, 25 μg of cRNA was fragmented. Each fragmented cRNA (15 μg) was then hybridized to an Affymetrix U74Av2 GeneChip microarray. Hybridization, washing and scanning were performed according to the Affymetrix manual.

Data from the scanned chips were analyzed using Affymetrix MAS 5.0 software (Hubbell et al., 2002; Liu et al., 2002). The significance of differential expression was determined by the number of pairwise comparisons (out of nine total) having a significant change in the same direction. The cutoff for significance was a *P*-value of 0.0025 by Wilcoxon's Signed Rank test for each pairwise comparison. The fold-change values reported are the means±s.d. of the nine comparisons. The Hoxd genes were not included in the reported results, but detection of their differential expression served as controls for both the tissue samples and detection by the microarrays. Hoxd genes had the greatest fold changes measured, as much as 190-fold greater signal strength for *Hoxd13* when comparing wild-type and $HoxD^{Del1–13}$ forelimb samples. Candidate genes were prioritized into categories by the number of significant change comparisons, and were categorized secondarily by the fold change. Gene lists were further filtered by eliminating those candidates that were called absent in both genotypes by the MAS 5.0 analysis. In some cases, probe sets were eliminated from the analysis when extensive BLAST searching indicated that they were not specific for an individual gene. The raw data were also analyzed with other publicly available software, including dChip (Li and Hung Wong, 2001) and GCRMA (Wu et al., 2003). The results from these complementary analyses largely confirmed the lists of candidate genes obtained by MAS 5.0. According to MIAME guidelines (Brazma et al., 2003), the complete microarray dataset was deposited in the public data repository of the European Bioinformatics Institute (ArrayExpress) with accession number E-MEXP-257.

Quantitative real-time RT-PCR

Single-stranded cDNA templates for real-time RT-PCR analysis were synthesized from the same RNA pools used for the microarray analysis, and from independently derived and extracted secondary samples as described above. Sixty-five to 100 bp amplicons and Taqman probes were designed using Primer Express 2.0 software (Applied Biosystems). Primer pairs were tested and efficiencies were measured using standard curves from serial dilutions of cDNA. Primer pairs having greater than 88% efficiency were judged to be acceptable for subsequent measurements. Results and amplification efficiencies were comparable using either Taqman or Sybr Green. Specificity of Sybr Green reactions was determined by examination of product melting curves as described (Ririe et al., 1997). cDNA was PCR amplified in a 7900HT SDS System (Applied Biosystems) and raw threshold-cycle (Ct) values were obtained from SDS 2.0 software (Applied Biosystems). Relative quantities (RQ) were calculated with the formula $RQ=E^{-Ct}$ using efficiencies (E) calculated for each run with the DART-PCR algorithm, as described (Peirson et al., 2003). A mean quantity was calculated from triplicate PCR reactions for each sample, and this quantity was normalized to two (for primary samples) or three (for secondary samples) similarly measured quantities of normalization genes as described (Vandesompele et al., 2002). Normalized quantities were averaged for three replicates for each data point and represented as the mean±s.d. The highest normalized relative quantity was arbitrarily designated as a value of 1.0. Fold changes were calculated from the quotient of means of these normalized quantities and reported as ±s.d. The statistical significance of fold-changes was determined by a paired Student's *t*-test. Taqman PCR was used to quantify the expression of *Hoxa11*, *Papss2*, *Aldh1a2*, *Stra6*, *Msx2*, *Prrx1*, *Gfra2* and *Epha3*. Sybr Green PCR was used to quantify the expression of *Sgk*, *Gdf10*, *Odz4*, *Nr2f1*, *Pcdha*, *Foxp1*, *Shox2* and *Lisch7*. Control genes for normalization, *Rps9*, *Tbp* and *Tubb4*, were amplified either by Sybr Green or Taqman PCR, as appropriate for each run. Primers and probe sequences can be retrieved at: http://www.unige.ch/sciences/biologie/biani/duboule/index_st.htm.

In situ hybridization

All cDNA fragments used as whole-mount situ hybridization (WISH) probes were prepared by RT-PCR using E12.5 genital or limb bud RNA, with the exception of the *Hoxa11* probe (gift of Catherine Fromental-Ramain). Four hundred to 700 bp amplicons were designed with MacVector software (Accelrys) using publicly available GenBank cDNA sequences. Specificity of the primers and chosen cDNA fragment was confirmed by BLAST analysis. Specific primer sequences are listed on the website indicated above. The various cDNAs were cloned into the pGEM-T vector (Promega) and the correct identities of the cloned fragments were confirmed by restriction enzyme analysis. DIG-labeled antisense probes were prepared by in vitro transcription with SP6 or T7 polymerase (Promega). WISH using embryos fixed in 4% paraformaldehyde was performed according to standard procedures. Because sex-specific differences in external genitalia only begin to appear at E16.5 (Suzuki et al., 2002), the sex of embryos was not routinely determined. Nevertheless, in some cases the gender of embryos was determined by PCR as described (Lavrovsky et al., 1998) to confirm that the expression patterns were not sex-dependent. All images represent one representative staining of at least two replicates for each condition.

Results

We sought to identify genes regulated by HOXD proteins, while determining whether the comparable expression patterns of Hoxd genes in developing digits and genitalia regulated similar or different downstream developmental pathways. We analyzed developmental gene expression by microarray analysis, quantitative real-time RT-PCR and WISH analysis. Our primary genetic tool was the $HoxD^{Del1–13}$ mutant stock, in which all Hoxd genes are deleted (Spitz et al., 2001).

Absence of shared candidate genes in E12.5 distal limbs and genitals by microarray analysis

We chose to use samples from E12.5 embryos as a starting point for our analysis, as it is the first day in which the genital bud exists as a structure that can be reliably dissected, and because Hoxd gene expression is reaching high levels in both structures at this time (Fig. 1A). Also E12.5 embryos, unlike younger specimens, have presumptive autopods clearly distinguishable from more proximal domains.

Triplicate wild-type and $HoxD^{Del1–13}$ homozygote pools of E12.5 RNA were analyzed using Affymetrix microarrays that contain probe sets representing approximately 12,000 cDNAs. The resulting data sets allowed a total of nine comparisons between pools to be made for each type of tissue (Fig. 1B). Using the criteria described in Table 1, the best candidates were chosen by the number of comparisons in which differential expression was statistically significant, and by the magnitude of the fold change. Surprisingly, of the strongest candidates, in which at least seven out of nine comparisons showed significant differential expression, only four genes showed a greater than twofold change in expression (Table 1; first row). When the criteria were relaxed to include genes with a fold-change cutoff of 1.4-fold, only 13 more genes were identified with seven significant comparisons (Table 1; second row). A third, even less stringent category, yielded 28 more candidates in which the threshold for fold-change remained at 1.4-fold, but the

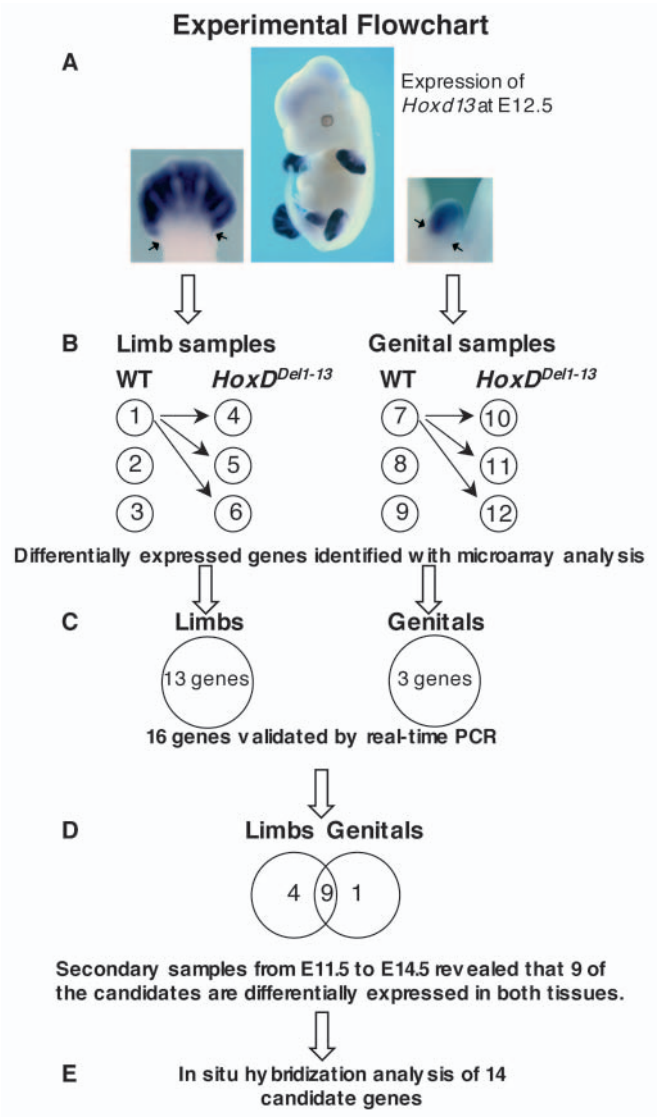

Fig. 1. Experimental strategy for identifying Hoxd-regulated genes in developing genitalia and forelimbs. (A) In situ hybridization of a wild-type E12.5 embryo stained with a *Hoxd13* probe illustrates the tissues dissected for this study. *Hoxd13* is strongly and broadly expressed in the genital bud (right) and distal forelimb (left). Genital buds and distal forelimb buds were dissected (arrows indicate cut points) from E12.5 wild-type (WT) embryos and from homozygous mutant embryos in which all nine Hoxd genes had been deleted ($HoxD^{Del1-13}$). (B) Gene expression was analyzed with Affymetrix microarrays (each array is represented schematically as a circle; see Materials and methods). (C) Microarray analyses yielded two sets of initially non-overlapping differentially-expressed candidate genes from limbs and genitals. A subset of the candidates (16 genes) was validated by quantitative real-time RT-PCR analysis. (D) Expression of the 16 candidate genes was measured by real-time RT-PCR over developmental time from secondary samples collected from E11.5 to E14.5. Nine out of 14 confirmed genes also had highly significant differential expression in the other tissue on at least one day of development. (E) The transcript profiles of the 14 genes were visualized by whole-mount in situ hybridization (WISH), in several cases further validating their differential expression.

number of significant differential comparisons was reduced to 6. Further relaxation of the criteria (Table 1; fourth row) expanded the list to hundreds of genes with less than six statistically significant comparisons. Strikingly, none of the candidate genes identified in the two tissues were found to be differentially expressed in both distal forelimbs and genitals.

Refinement by quantitative real-time RT-PCR

The small fold changes observed made it crucial to further verify the potential differentially expressed genes by RT-PCR. We chose to validate a subset of 25 genes, including all four from the most stringent category, most from the second category (10 out of 13), and a sample of 11 genes from the two least restrictive categories. We first quantified expression of these 25 genes in our primary E12.5 samples that were used for the microarray analysis. Of these 25 genes, 16 showed a differential expression by real-time RT-PCR that was similar to that observed by microarray analysis (Fig. 1C). Our threshold for defining a gene as 'validated' was a change of at least 1.4-fold by RT-PCR, in the same direction as was detected by the microarray analysis. The precise fold changes measured for validated genes are indicated in Tables 2 and 3. The percentage of candidates confirmed from the two most stringent categories in Table 1 was 78% (11 out of 14). By contrast, only 5 out of 11 (45%) genes were confirmed from the two least stringent categories, thus supporting the use of these categories to identify the most likely candidates. Nonetheless, apparent false-positives from the microarray analysis were found in each category, emphasizing the need to verify any specific gene before being assured of its differential expression.

Table 1. Summary of microarray analysis and real-time RT-PCR verification

Criteria		Genes detected			Number tested by RT-PCR	Number of confirmed 1° samples	Number of confirmed 2° samples
Fold change	*n*/9*	Limbs	Genitals	Total			
>2.0-fold	≥7	1	3	4	4	3 (75%)	3 (75%)
>1.4<2.0-fold	≥7	7	6	13	10	8 (80%)	7 (70%)
>1.4-fold	6	12	16	28	8	4 (50%)	3 (37%)
>1.4-fold	<6	>100	>100	>200	3	1 (33%)	1 (33%)
Total					25	16	14

*Number of nine pairwise comparisons showing a significant increase or decrease (P<0.0025) by Wilcoxon's Signed Rank Test.
1° samples, cDNA made using the same RNA that was used to produce cRNA for microarray hybridization.
2° samples, independently extracted, triplicate RNA samples used to make cDNA.
RT-PCR, quantitative real-time reverse-transcription PCR.

Table 2. Differentially expressed genes initially identified by comparing wild-type and *HoxD*$^{Del1\text{-}13}$ E12.5 genital buds

Gene symbol	Affymetrix probe set ID	Fold change (FC) microarray	*n*/9	1° sample FC by RT-PCR	2° sample FC by RT-PCR at E12.5	Most significant FC in limbs by RT-PCR
Genes with lower expression in *HoxD*$^{Del1\text{-}13}$-mutant genitals:						
Gfra2	92449_at	2.26±1.99	7	1.59†	2.08±0.29**	1.63±0.23 at E14.5**
Sgk	97890_at	1.83±0.26**	9	1.66±0.36**	1.54±0.17**	2.36±0.18 at E11.5**
Gene with higher expression in *HoxD*$^{Del1\text{-}13}$-mutant genitals:						
Hoxa11	104021_at	2.16±0.64**	9	2.07†	2.22±0.41**	1.34±0.18 at E11.5*

All values are the means of three replicates ±s.d.
*P-value for paired Student's t-test<0.05; **P-value<0.01.
n/9, RT-PCR, 1°, 2° samples as in Table 1.
†Only one comparison possible (original material limiting).

Table 3. Differentially expressed genes initially identified by comparing wild-type and *HoxD*$^{Del1\text{-}13}$ E12.5 distal forelimb buds

Gene symbol (synonym)	Affymetrix probe set ID	Fold change (FC) microarray	*n*/9	1° sample FC by RT-PCR	2° sample FC by RT-PCR at E12.5	Most significant FC in genitals by RT-PCR
Genes with lower expression in *HoxD*$^{Del1\text{-}13}$-mutant forelimbs						
Papss2	96713_at	1.79±0.72*	7	1.63±0.57	1.51±0.17**	1.83±0.35 at E14.5**
Aldh1a2 (*Raldh2*)	101707_at	1.66±0.33*	7	1.71±0.28**	1.54±0.15**	None
Stra6	102258_at	1.66±0.47	4	1.52±0.53	1.56±0.34*	None
Nr2f1 (*Coup-TF1*)	102715_at	1.56±0.20**	7	1.54±0.12**	1.56±0.20**	–2.02±0.35 at E14.5**
Gdf10	160860_at	1.43±0.46	7	1.55±0.57	1.79±0.24**	2.66±0.76 at E12.5**
Foxp1	96183_at	1.44±0.22*	6	1.64±0.32**	1.43±0.31	None
Lisch7	99452_at	1.41±0.16**	6	1.42±0.05**	1.20±0.17‡	1.25±0.07 at E13.5**
Genes with higher expression in *HoxD*$^{Del1\text{-}13}$-mutant forelimbs						
Epha3 (*Mek4*)	95298_at	2.06±0.34**	9	1.73±0.43*	1.55±0.22**	1.75±0.12 at E13.5**
Odz4	98313_at	1.80±1.01	6	1.46±0.30	1.65±0.26**	1.47±0.24 at E14.5**
Shox2 (*Og12x*)	99042_s_at	1.62±0.50	7	1.44±0.54	1.59±0.48*	1.33±0.20 at E13.5*
Pcdha† (*Cnr1-8*)	160610_at	1.61±0.32*	7	1.57±0.31*	1.62±0.40*	–1.29±0.05 at E13.5**

All values are the means of three replicates ±s.d.
*Paired Student's t-test P<0.05; **P-value<0.01.
n/9, RT-PCR, 1°, 2° samples as in Table 1.
–FC, change in opposite direction from microarray.
†This probe set is specific for the constant portion of the *Pcdha* gene cluster (Sugino et al., 2000), so all isoforms of *Pcdha* should be detected.
‡The differential expression of *Lisch7* was less than 1.4-fold in these secondary samples, but it was maintained on the list because it was significantly different at both E13.5 and E14.5.

Shared HOXD-dependent genes in digits and genitals are time-delayed

Results comparing samples from E12.5 indicated that there were no common Hoxd-target candidate genes in distal limbs and genitalia. However, because the genital eminence starts to develop 1 to 2 days later than the forelimb, we analyzed and compared samples obtained from different stages of development, reasoning that shared molecular mechanisms could be implemented at different times in both structures. For this reason, and to further confirm the differential expression seen in our primary samples, we used real-time RT-PCR to analyze secondary samples from embryos at days E11.5 to E14.5 to generate a developmental time course of expression in genitals and distal forelimbs for each of the 16 candidate genes and two control genes. If a candidate gene were involved in digit or genital bud formation, we expected that its differential expression would be detected during this time period because digit morphogenesis is essentially complete by E14.5 and the genital bud is a well-developed structure at this time.

Because the same secondary RNA samples were to be used to characterize all candidate genes, we first assayed for any systematic differences amongst samples. Accordingly, we chose two genes, *Prrx1* and *Msx2*, which showed no significant difference in expression by microarray analysis. Furthermore, these particular genes served as robust controls for either random or systematic effects, as both are expressed in the same mesenchymal tissues as the Hoxd genes and function in limb patterning (Leussink et al., 1995; Satokata et al., 2000). The resulting real-time RT-PCR expression profiles for these control genes indicated no differential expression in either forelimb or genital buds (see Fig. S1 in the supplementary material), supporting the use of these samples in identifying truly differentially expressed genes.

We confirmed differential expression at E12.5 for 14 out of the 16 genes in the secondary samples, giving a final list of 14 validated candidate genes (Tables 2 and 3). Therefore, despite the relatively small fold changes detected, multiple rounds of verification of these genes rigorously confirmed their differential expression. Furthermore, among the 11 candidates identified in distal limbs, seven also had highly significant (P<0.01) differential expression in genital buds on at least one day of development (Table 3; last column). With the exception of *Gdf10*, the most significant differential expression in genitals was found in embryos older than 12.5 days (the

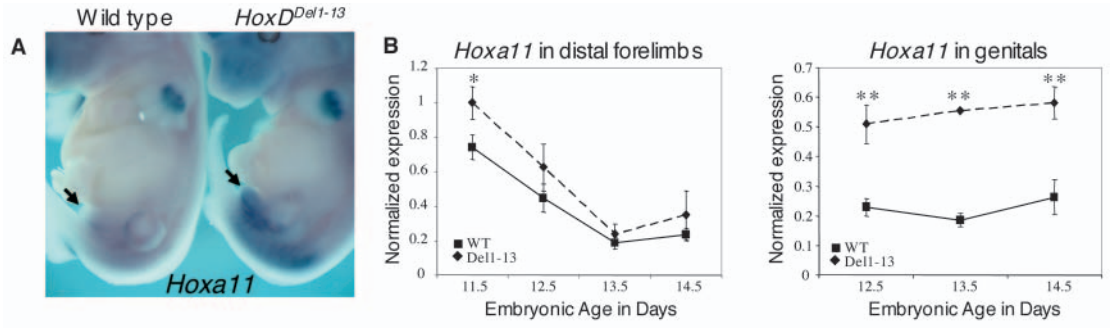

Fig. 2. *Hoxa11* is upregulated in genital buds when Hoxd genes are fully deleted. (A) WISH reveals an upregulation of *Hoxa11* in the genital bud (arrows) of an E12.5 embryo. Upregulation is also apparent in the trunk, whereas it is not obvious in the forelimbs. Hindlimbs were removed to visualize the genitalia. (B) Real-time RT-PCR analysis confirms that *Hoxa11* is expressed 2- to 3-fold higher in developing $HoxD^{Del1–13}$ genitalia from E12.5 through E14.5. By contrast, *Hoxa11* is only slightly increased in mutant forelimbs, to a level that is statistically significant at E11.5 only (1.35-fold). For these and all graphs in other figures: *Paired Student's *t*-test $P<0.05$; **P-value<0.01. Values are means of triplicate samples; error bars represent s.d.

differential expression of *Gdf10* in E12.5 genitals was apparently not detected by the microarrays because of its weak signal). Similarly, of the three candidates initially identified in genitals, two also had highly significant differential expression in limbs (Table 2; last column) at stages other than E12.5. Ultimately, nine out of the 14 candidate genes were found to be differentially expressed in both presumptive digits and genitals.

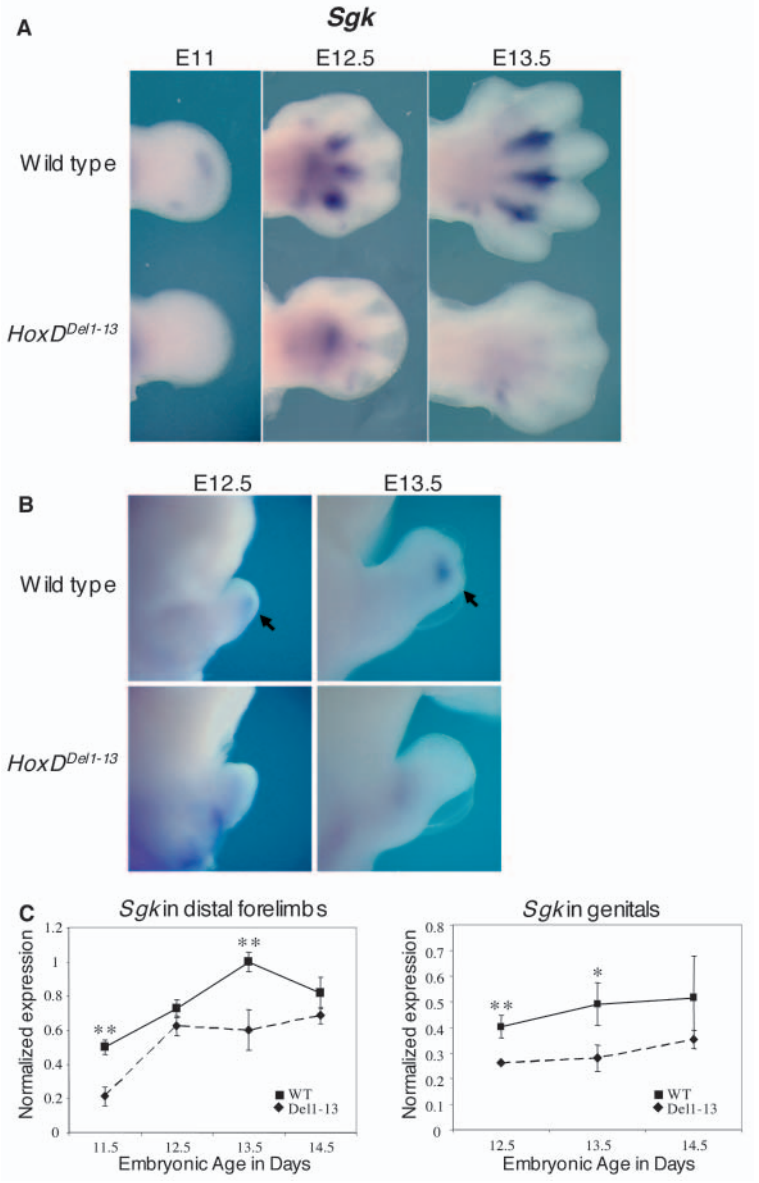

HOXD-dependent differential expression of *Hoxa11*, *Sgk* and *Gfra2*

After quantifying variations in the RNA levels of these candidate target genes over developmental time, we investigated their spatial expression patterns. We designed WISH probes for each of the 14 candidate genes and stained wild-type and mutant embryos at the appropriate stages. The three genes initially identified as differentially expressed in genitals (Table 2) were among the most clearly confirmed. Firstly, although *Hoxa11* was barely detectable in wild-type E12.5 genital buds by WISH, it was consistently upregulated in both the genital bud and trunk of the $HoxD^{Del1–13}$ mutant specimens (Fig. 2A). This observation confirmed the stable 2- to 3-fold elevation in *Hoxa11* expression measured in $HoxD^{Del1–13}$ genital buds by real time RT-PCR (Fig. 2B). By contrast, only a slight 1.3- to 1.4-fold increase in *Hoxa11* expression was measured in $HoxD^{Del1–13}$ limbs.

Contrastingly, the *Sgk* (serum glucocorticoid-regulated kinase) and *Gfra2* (glial cell line-derived neurotrophic factor family receptor alpha 2) genes

Fig. 3. Expression of *Sgk* is dependent on Hoxd gene function in genitals and forelimb buds. (A) *Sgk* expression appears distally in E11 wild-type limb buds. At E12.5 and E13.5, expression is prominent in the proximal portion of the interdigital zone. By contrast, *Sgk* expression in mutant $HoxD^{Del1–13}$ limbs is largely limited to a proximal domain at E12.5, with little interdigital staining. (B) In the developing genital bud, *Sgk* is expressed in a distal domain of the ventral mesenchyme, adjacent to the urethral epithelium (arrow). This domain is not visible in mutant genital buds. (C) Real-time RT-PCR measurements mirror the WISH results, with highly significant (**$P<0.01$) differential expression in both limbs and genitals. Although the differential expression was initially detected in genitals, the highest fold change in the developmental series was measured in limbs (2.36-fold at E11.5).

clearly showed significant downregulation in both $HoxD^{Del1–13}$ limbs and genitals. The downregulation in the expression of *Sgk* was initially detected by microarray in E12.5 genital buds. Upon WISH staining, differential expression was also clearly apparent in forelimb buds (Fig. 3A). *Sgk* expression first appears in a distal domain of the forelimb bud at E11. This domain was not observed in three out of three stained $HoxD^{Del1–13}$ E11-E11.5 embryos. The differential expression at E11.5 was quantified as being 2.3-fold by real-time RT-PCR (Fig. 3C). At E12.5, some expression did appear in $HoxD^{Del1–13}$ forelimbs (Fig. 3A; second panel), but only proximally, whereas a more distal interdigital domain developed in wild-type forelimbs. The proximal domain in the center of the $HoxD^{Del1–13}$ E12.5 autopod may explain why differential expression was not detected in E12.5 limbs by microarray analysis, or by real-time RT-PCR (Fig. 3C). At E13.5, the differential expression was again significant, as the strong interdigital domain seen in wild-type limbs was never scored in $HoxD^{Del1–13}$ limbs. Differential expression of *Sgk* was no longer detected at E14.5, but by this time the interdigital domain of expression in wild-type forelimbs had disappeared (data not shown). A similar distal domain of *Sgk* expression was seen in wild-type genital buds from E11.5 (data not shown) through to E13.5, which was not observed in $HoxD^{Del1–13}$ genitals (Fig. 3B).

Similar to *Sgk*, *Gfra2* expression was visibly reduced in both $HoxD^{Del1–13}$ mutant forelimbs and genital buds (Fig. 4). In contrast to *Sgk*, however, differential expression of *Gfra2* was apparent first in genitalia and later in limbs, as seen both by WISH and real-time RT-PCR analysis. Robust expression of *Gfra2* never developed in $HoxD^{Del1–13}$ forelimbs, at least not through E14.5, whereas a clear signal was observed in wild-type limbs at E13.5, and then only in the ventral mesenchyme of the autopod (Fig. 4A). The differential expression was first detected in genitals at E11.5 (not shown) and continued through E14.5 (Fig. 4B). Although *Gfra2* expression did not disappear in $HoxD^{Del1–13}$ genitalia, it was clearly reduced and restricted to a more distal domain.

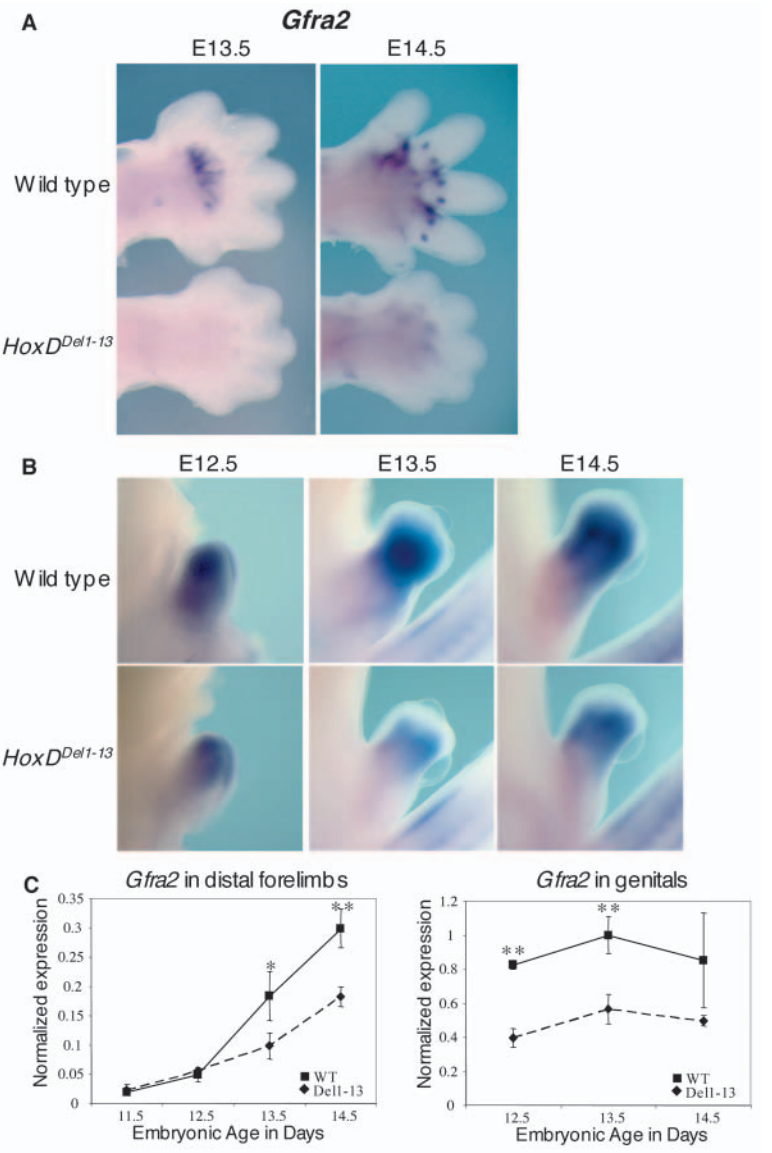

Fig. 4. *Gfra2* is downregulated in limbs and genitals in the absence of Hoxd gene function. (A) Ventral view of *Gfra2* expression in right forelimbs. *Gfra2* expression is first visible at E13.5 on the ventral side of the developing autopod. This domain is only weakly stained in $HoxD^{Del1–13}$ mutants. (B) *Gfra2* is expressed strongly in the genital bud from the time of its emergence. By E13.5, the expression is much stronger in the distal half of the bud. In mutant genitalia, the expression is reduced and is more distally restricted at all days stained. (C) Real-time RT-PCR analysis quantifies and confirms the differences observed by WISH.

Odz4 and Epha3 are downregulated by Hoxd gene products

The expression patterns of all of the candidate genes in Table 3 were determined (Fig. 5, see also Figs S2-S4 in the supplementary material) for the developmental stages in which they showed significant differences by real-time RT-PCR. *Odz4* and *Epha3* RNA levels were increased in both $HoxD^{Del1–13}$ limbs and genitals (Fig. 5A,B), suggesting that they could be targets for Hoxd repression (as are *Shox2* and *Pcdha*, see Fig. S4C,D). The increase in *Odz4* and *Epha3* expression in mutant forelimbs was clearly detected by WISH. At E12.5, the domain of *Odz4* expression increased both in its distal extent and intensity, and this increase was still visible in E13.5 and E14.5 embryos (not shown). Similarly, the domain of *Epha3* expression extended slightly more distally, and was reinforced towards the posterior and proximal parts of mutant digits at E12.5 (Fig. 5B). An increase of *Odz4* and *Epha3* in genitals was difficult to visualize by WISH, but was highly significant ($P<0.01$) by real-time RT-PCR in both cases (Fig. 5A,B).

Candidates target genes for Hoxd activation in distal forelimb

In contrast to *Odz4* and *Epha3*, *Gdf10* is a candidate for Hoxd upregulation (as are the six other genes initially identified in

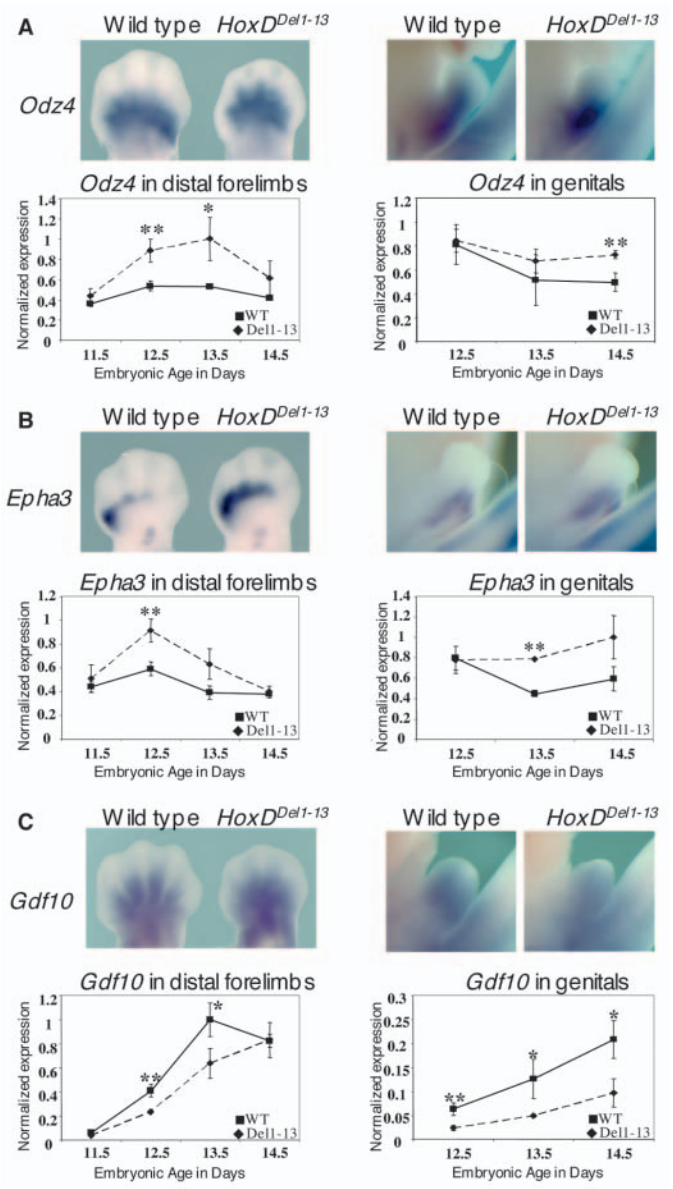

Fig. 5. Analysis of candidates for downregulation (*Odz4* and *Epha3*) or upregulation (*Gdf10)* by Hoxd gene products. WISH staining of E12.5 right forelimbs are shown for each gene. Lateral views of genitals (at right in each panel) are at E13.5 for *Odz4* and *Epha3*, and E12.5 for *Gdf10.* Real-time RT-PCR quantification for each gene is shown as graphs. (A) The *Odz4* forelimb expression domain extends more distally in $HoxD^{Del1–13}$ mutants at E12.5, and expression is gained in the mutant genitalia. (B) *Epha3* is expressed at a higher level in mutant forelimbs. The limb expression domain increases posteriorly (right) and distally, when compared with the wild type (left). Real-time RT-PCR measurements also indicate an increase in genital expression in the $HoxD^{Del1–13}$ mutant (**P<0.01 at E13.5). By WISH, this increase is visualized as a slight broadening of the expression domain in the mutant genitals. (C) *Gdf10* expression is weaker in mutant forelimbs and genital buds. *Gdf10* is expressed in a broad domain in both wild-type and mutant limbs and genitals, making visualization of differences by WISH difficult, although some decrease in mutant tissues is apparent. Real-time RT-PCR quantification shows highly significant differences (**P<0.01) in both tissues.

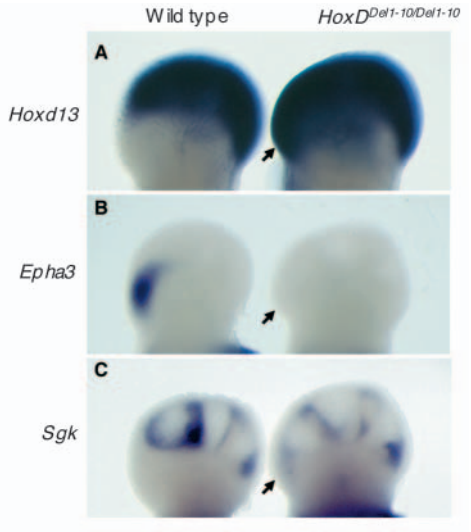

Fig. 6. Analysis of *Epha3* and *Sgk* expression in the $HoxD^{Del1–10}$ gain-of-function mutant. (A) Anterior gain of *Hoxd13* expression (arrow) in an E11.5 $HoxD^{Del1–10}$ right forelimb. (B) *Epha3* expression is completely abolished in the region where *Hoxd13* expression is gained (arrow). This observation contrasts with the increased *Epha3* expression seen in $HoxD^{Del1–13}$ mutant limbs (Fig. 5B), further supporting *Epha3* as a candidate gene for Hoxd repression. Complete *Epha3* repression was observed in 11 out of 12 $HoxD^{Del1–10}$ forelimbs stained. (C) By contrast, *Sgk* expression is gained in the region of presumptive digit 1 (arrow) in the $HoxD^{Del1–10}$ forelimb. This weakly stained domain was visible in eight out of eight mutant E11.5 forelimbs. Accordingly, *Sgk* expression was lost in the E11.5 $HoxD^{Del1–13}$ mutant (see Fig. 3A), indicating that *Sgk* is upregulated by Hoxd gene expression.

limbs listed in Table 3). Because *Gdf10* is expressed broadly in both forelimbs and genital buds from both genotypes, its loss of expression in the $HoxD^{Del1–13}$ mice was difficult to document by WISH (Fig. 5C), although the difference was highly significant by real-time RT-PCR in both tissues. For other genes, such as *Papss2* (see Fig. S2A in the supplementary material) and *Aldh1a2* (see Fig. S3A in the supplementary material), the in situ staining confirmed the differential expression as quantified by microarray and real-time PCR, but their expression patterns were so dynamic that an interpretation of their role downstream of Hoxd was difficult. The patterns of the remaining six genes confirmed to varying degrees the differential expression (see Figs S3, S4 in the supplementary material).

Genetic validation of HOXD regulation of *Epha3* and *Sgk*

In order to further validate *Epha3* and *Sgk* as candidate target genes, we made use of additional mouse strains with specific Hox gain or loss of functions. In the case of *Epha3*, its expression in the most anterior part of the developing hand-plate was virtually exclusive from Hoxd gene expression in digits, suggesting a repression of the former by the latter products. We tested this possibility by using a mouse strain showing a gain of function of *Hoxd13* and *Hoxd12* in distal limbs ($HoxD^{Del1–10}$) (Zakany et al., 2004). In $HoxD^{Del1–10}$ mice, the expression of *Hoxd13* in presumptive digits is extended anteriorly, thus overlapping with the *Epha3* domain (Fig. 6A).

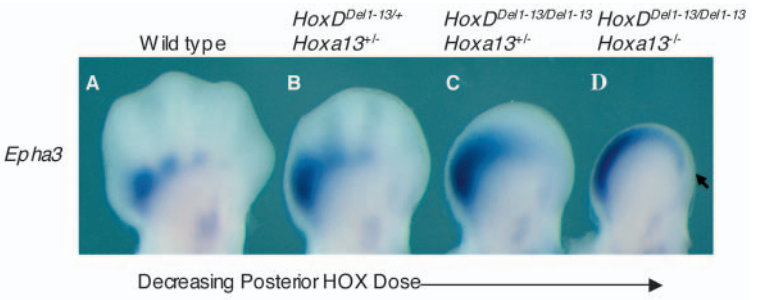

Fig. 7. *Epha3* expression in combined *Hoxa13*/Hoxd mutants. WISH staining of right forelimbs from E12.5 littermates; anterior is to the left and posterior to the right. (A) Wild-type *Epha3* expression pattern at E12.5. (B) *Epha3* expression in transheterozygote littermate, where one copy each of *Hoxa13* and the Hoxd cluster are intact. *Epha3* expression is moderately gained similar to that seen when both copies of the Hoxd cluster are deleted (Fig. 5B). (C) The gain of *Epha3* expression spreads through much more of the autopod, distally and posteriorly, when a single *Hoxa13* is inactivated in combination with a homozygous deletion of the Hoxd cluster. (D) *Epha3* expression in a double homozygote limb. Even though most of the autopod does not form in this mutant, *Epha3* expression is gained to the posterior extreme of the limb bud (arrow). Because of the small size of the mutant limbs, it is useful to compare with the expression in E11.5 embryos to illustrate the gain of expression (as shown in Fig. 6B).

In the $HoxD^{Del1–10}$ mutant limbs, expression of *Epha3* was no longer detected, concomitantly with a strong gain of *Hoxd13* expression in the same domain (Fig. 6B). This result confirmed the repressive effect of Hoxd gene products over *Epha3* transcription, in agreement with the observed gain of expression of *Epha3* in limbs lacking all Hoxd function (Fig. 5B). In this latter case, *Epha3* expression did not extend throughout developing digits, which normally express posterior Hoxd genes (Fig. 5B), suggesting that Hoxd gene products cannot be the only proteins preventing *Epha3* expression in developing distal limbs.

Functional redundancy between Hoxa and Hoxd genes in limb and genital development is well established (e.g. Kondo et al., 1997; Fromental-Ramain et al., 1996; Davis et al., 1995). *Hoxa13*, in particular, is strongly expressed during digit development, in a domain largely overlapping with that of posterior Hoxd genes. In addition, the most distal digit domain where *Epha3* expression was not gained in the absence of Hoxd gene functions precisely coincides with the *Hoxa13* transcript domain (Fig. 5B). Therefore, we tested whether the *Epha3* gain of expression would be enlarged upon inactivation of the *Hoxa13* gene in combination with the absence of Hoxd genes. *Epha3* expression was gained in mutant forelimbs in a Hox-dose dependent fashion (Fig. 7). When one copy of *Hoxa13* was inactivated in combination with a Hoxd-homozygous deletion, a much larger distal and posterior gain in *Epha3* expression was scored than in the Hoxd mutant alone (Fig. 7C, compare with Fig. 5B). When the remaining copy of *Hoxa13* was also inactivated so that the only Hox products present in the autopod were from the *Hoxa11* gene, the expression domain of *Epha3* was further gained to the posterior margin of the forelimb bud (Fig. 7D). Therefore, *Epha3* appears to be downstream of both the Hoxa and Hoxd genes.

The gain of expression of posterior Hoxd genes in $HoxD^{Del1–10}$ mutant mice was also used to monitor expression of the *Sgk* gene, a candidate for transcriptional upregulation by Hoxd gene products. Unlike *Epha3*, *Sgk* expression in wild-type developing digits perfectly overlaps with that of *Hoxd13* (Fig. 6; compare A with C). In particular, *Sgk*, like *Hoxd13*, was not detected in the most anterior aspect of the developing distal limb (Fig. 6). In mutant $HoxD^{Del1–10}$ limbs, however, *Sgk* expression was detected concomitantly with the gain of expression of *Hoxd13* in this anterior domain (Fig. 6A). This confirms the results obtained with both microarray and RT-PCR analyses, which placed *Sgk* downstream of HOXD function.

Discussion

Searching for HOX-regulated genes

Although HOX proteins were amongst the first transcription factors whose genes were isolated in higher eukaryotes, very few Hox target genes have been described so far. This apparent paradox finds its roots in the functional history of this gene family. In the course of evolution, different Hox genes were co-opted to achieve a variety of functions in different organs or structures. Therefore the functional redundancy varies quite dramatically in different structures and reflects the phylogeny of this gene family (Duboule and Wilkins, 1998). For instance, a late co-option of a few Hox genes in a defined organ will result in a low level of redundancy, with only some genes being functional. By contrast, the ancestral functional domain of this gene family, i.e. the developing trunk, will display a maximum of redundancy, making functional approaches difficult.

An intermediate situation is observed in both limbs and genitalia, where mostly two clusters (Hoxa and Hoxd) are involved in patterning. Consequently, the level of functional redundancy observed in these structures is probably not as important as that in the developing trunk, and removing the functions of two orthologous genes leads to drastic alterations. Therefore, the search for target genes should, in principle, be easier in developing limbs and genitalia than in the developing spinal cord or sclerotomes. This is, however, not necessarily the case, as removing Hox gene functions progressively deletes the corresponding limb and genital structures, rather than inducing distinct morphological alterations.

We tried to overcome this problem by using an intermediate genetic condition in which the limbs and genitalia, while being affected in their overall size and patterning, still display fairly good morphologies due to the function of the remaining Hoxa genes. Because limbs and genitals have comparable early developmental phases, we wondered whether their different morphological fates could be accounted for by distinct transcriptional outputs following the activation of the same Hox genes, i.e. whether the same HOX proteins would trigger the activation of different genetic programs.

Distal limbs and genitals share common genes downstream of Hoxd function

We identified and validated 14 genes as potential HOXD targets. Six of these (*Hoxa11*, *Sgk*, *Gfra2*, *Epha3*, *Odz4* and *Gdf10*) are especially strong candidates. Interestingly, with the exception of *Hoxa11*, these genes are similarly regulated in

limbs and genitals, which further indicates that these two structures display closely related developmental strategies. Initially, these genes were not found to be regulated simultaneously in both developing buds, until the analyses were extended to various time-points. This revealed that the same variations in gene regulation were observed in both structures, but usually slightly later in genitalia than in limb buds (*Gfra2* is an exception to this trend, see below). This observation nicely fits the developmental delay that exists between these buds, as the genital eminence emerges with a one to two day delay with respect to forelimb budding.

Strikingly, except for *Hoxa11*, the function of the five other potential target genes has not yet been fully explored in limb or genital development. In fact, none of the 14 candidate genes are members of the classical FGF, BMP, WNT or SHH signaling pathways. Only the retinoid pathway (*Aldh1a2*, *Stra6*) is represented among the candidates. This observation supports the conclusion that, at the developmental stages we analyzed, the Hoxd genes act downstream or independently of most of the previously described limb and genital patterning pathways.

Regulatory crosstalk between Hox clusters

Post et al. (Post et al., 1999) previously reported that the expression domain of *Hoxa11* extends more distally into the autopod domain when *Hoxa13* is mutated. We have found a similar upregulation of *Hoxa11* in genitals devoid of Hoxd gene function. Therefore *Hoxa11* is a common downstream target of Hox proteins. In our study, *Hoxa11* did not increase significantly in forelimbs, probably because of the presence of the *Hoxa13* product. As *Hoxa13* is also expressed in developing genitals, it is unclear why we observe a clear increase in *Hoxa11* transcripts in the absence of Hoxd genes. Nonetheless, the combined results from our study and the findings of Post et al. (Post et al., 1999) identify *Hoxa11* as similarly regulated by Hox proteins in limbs and genitals. In both cases, one may wonder whether such an upregulation of *Hoxa11* could both weaken the phenotype and, accordingly, reduce the changes seen in the expression of candidate target genes through functional compensation.

Despite this clear effect on *Hoxa11* regulation and a few other reported cases of auto-regulation (Popperl et al., 1995; Popperl and Featherstone, 1992), cross-regulatory and auto-regulatory interactions amongst Hox genes and their products does not appear to be the rule, particularly for those posterior Hoxd genes involved in limb and genitalia development. This is demonstrated well by the inability of Hoxd transgenes to be faithfully expressed in distal limbs and genitalia whenever integrated outside the Hoxd cluster, even in the presence of the full Hox gene complement (see van der Hoeven et al., 1996).

Sgk in limb and genital development

The *Sgk* gene is certainly amongst the more unlikely candidates identified in this work. No developmental role for this kinase has been reported, even though the *Sgk* orthologous gene in *C. elegans* has been identified as a critical determinant of life span and stress response (Hertweck et al., 2004). A previous study reported tissue-specific expression of *Sgk* during development, but an analysis of limbs beyond E10.5 was not described, thus overlooking the expression phase starting at E11.5 (Lee et al., 2001). The mouse genome encodes two other *Sgk* isoforms (*Sgk2* and *Sgk3*), which is likely to account for the virtual absence of a phenotype in mice null for the gene (Wulff et al., 2002).

Among protein kinases, the SGK family is most closely related to the AKT protein kinases. A developmental role for AKT kinases was not fully evident until null mutations for *Akt1* and *Akt2* were combined (Peng et al., 2003). Likewise, the developmental role of the *Sgk* genes will probably require detailed combined analysis of all three forms. Because both AKT and SGK kinases act downstream of PDK1 (3-phosphoinositide-dependent protein kinase 1), SGK could participate in the recently reported involvement of AKT in the regulation of apoptosis in the limb (Kawakami et al., 2003). Biochemical studies have shown that SGK has an anti-apoptotic function (reviewed by Lang and Cohen, 2001), at least partially through its phosphorylation and inactivation of the pro-apoptotic transcription factor FKHRL1 (Brunet et al., 2001; Mikosz et al., 2001). Intriguingly, the domain of *Sgk* expression we report, especially at E13.5 (Fig. 3), is adjacent to the domain of interdigital cell death occurring more distally (Chen and Zhao, 1998). Likewise, a domain of apoptosis has been reported in the distal genital bud (Haraguchi et al., 2001; Suzuki et al., 2003), immediately adjacent to the domain of *Sgk* expression. SGK could be involved in regulating the domains of apoptosis or proliferation in both structures and its mis-regulation could contribute to the smaller size of appendages seen in the $HoxD^{Del1–13}$ mutant.

Gfra2 and the innervation of distal structures

Gfra2 codes for a receptor for the neutrophic factor neurturin, which signals through the RET receptor tyrosine kinase (Buj-Bello et al., 1997). A null mutation in this gene caused defective parasympathetic innervation of the gut and penis (Laurikainen et al., 2000; Rossi et al., 1999) but, as for *Sgk*, the existence of closely related family members makes full assessment of the developmental role difficult. We report here that the *Gfra2* gene is highly expressed from the onset of genital budding, an expression that is markedly diminished in the absence of Hoxd genes. Although the expression pattern correlates with the role in the innervation of the genitalia, the breadth of *Gfra2* expression throughout the genital bud suggests an additional developmental role as well. The expression outside of purely neuronal tissue has been previously noted, but as yet no function has been assigned (Klein et al., 1997).

The *Gfra2* expression pattern we report in limbs is significantly more restricted than that in genitals, but is equally Hoxd dependent. In contrast to most of the other candidates, differential expression of *Gfra2* appears later in limbs than in genitals. The only function for *Gfra2* that has been reported in limbs is a postnatal requirement for the innervation of sweat glands on the ventral surface of the paws (Hiltunen and Airaksinen, 2004). Although this function is likely to be required too late in development to be assigned to the expression we see at E13.5-14.5, it suggests a possible role in the innervation of this domain of the limb.

Eph genes as Hox targets?

Ephrins and their receptors have a well-established role in neuronal pathfinding, cell migration and cell adhesion (reviewed by Poliakov et al., 2004). Their role in limb development has only recently begun to be explored, but the

redundancy and overlapping expression domains of the ephrin and Eph genes (eight and 13 family members, respectively) makes this task particularly challenging. Compagni et al. showed that females heterozygous for a null mutation of ephrin B1 have digit duplications and bifurcations (Compagni et al., 2003). Stadler et al. initially established a link between Hox gene expression and ephrin signaling by showing that *Epha7* expression is markedly lower in *Hoxa13*-null forelimbs (Stadler et al., 2001). Another study showed that over-expression of ephrin A2, one of the ligands of EPHA3, caused digit bifurcations and fusions in chick limbs (Wada et al., 2003).

In addition, previous studies have reported that ephrin receptor (Eph) genes are the direct targets of Hox proteins. HOXA9 has been shown to directly bind to and regulate the expression of the *Ephb4* gene in cultured endothelial cells (Bruhl et al., 2004). Similarly, when co-expressed in vitro along with PBX1, HOXA1 and HOXB1 bind to and activate transcription from an enhancer sequence that is known to direct rhombomere-specific expression of *Epha2* (Chen and Ruley, 1998). Taken together these studies clearly establish a link between Hox genes and ephrin signaling.

Our data show that Hoxd and Hoxa genes act in combination to downregulate *Epha3* expression in developing digits. However, the biological relevance of this repression is unclear in part because *Epha3*-null mice have no abnormal phenotype (Vaidya et al., 2003). Our microarray data indicate that at least 12 of the ephrin and Eph genes are expressed in developing limbs and genitals. Therefore, defining a precise role for Eph and ephrin genes in limb development will require comprehensive studies of all of these genes. Regardless of its function, the *Epha3* gene can serve as a model for Hox regulation, as demonstrated by its complementary expression response in three kinds of Hox mutant stocks.

A horizontal regulatory strategy

Like the Hox genes themselves, all of the best candidate genes identified have multiple paralogs in the mouse genome, suggesting that functional redundancy may prevent the rapid elucidation of the biological role of the downstream genes. This complex situation is not unexpected considering the global function of Hox genes during vertebrate development, which is to modulate the fate of a given morphological module, rather than triggering the activation of novel genetic pathways. For example, the difference between a cervical and a lumbar vertebra is most likely to be due to subtle modulations of the same genetic determinants, rather than to the function of distinct pathways. In the case of both the limbs and genitalia, Hox genes participate in both the elaboration and the specification of the structures, and therefore affect the entire process rather than some specific parts of it.

In this view, the difficulty to assign clear target genes to the Hox proteins, at least during trunk, limb and genital development, is not surprising, but may be a precise indication of how the system works. This 'horizontal' regulatory strategy, whereby subtle variations in the amounts of related proteins impact upon the balance between a large set of products is in marked contrast with the situation found in arthropods, where Hox genes seem to be part of more 'vertical' regulatory processes. In the former case, various thresholds of target production, or combinations thereof, may induce a structure to produce a given morphology rather than another, related one. In the latter case, the presence or absence of a Hox product may trigger a chain of events leading to the choice of a given genetic pathway.

The vertebrate case will be difficult to solve with our current analytical tools, given the difficulty of identifying global correlations out of multiple parameters, rather than punctual downstream effectors. The analysis of HOX protein-binding sites may help to some extent, but in vitro studies have shown that Hox proteins by themselves bind DNA rather nonspecifically, using core-binding sequences of only four nucleotides (Phelan and Featherstone, 1997). The binding specificity apparently comes from Hox proteins forming complexes with other proteins, including those of the Pbx and Meis gene families, each with their own binding specificities. Indeed recent work in *Drosophila* has shown that a complex of at least five protein subunits represses the well-characterized Hox target gene *Distalless* (Gebelein et al., 2004). While some of the binding sites for higher order complexes on mammalian DNA have been determined (reviewed by Mann and Affolter, 1998), it is as yet difficult to reconcile these in vitro studies with the in vivo evidence. In particular, we do not know which complexes function in limbs and genitals, especially since MEIS1, which has been reported to be the strongest in vitro binding partner for *AbdB*-related HOX proteins (Shen et al., 1997), is not expressed in distal limbs (Mercader et al., 1999). Therefore, although some of the genes identified here could be direct Hox targets, demonstrating this conclusively will require future studies of the Hox transcription complexes in limbs and genitals. When appropriate antibodies become available, chromatin-immunoprecipitation experiments will be invaluable for conclusively demonstrating Hoxd interactions with specific regulatory regions. Our study provides a list of genes that can serve as substrates for these future studies.

We thank J. Zákány for mutant mice and consultations. The assistance of P. Descombes, M. Docquier, O. Schaad and D. Chollet (NCCR Genomics Platform) was essential for our microarray and real-time PCR analysis. In addition we thank P. Descombes and M. McDonald for critical reading of the manuscript, sharing reagents and help with data analysis; M. Kmita for discussions and generous sharing of mutant embryos; T. Montavon for sharing reagents; and P. Chambon for providing *Hoxa13*-mutant mice. This work was supported by funds from the Canton de Genève, the Claraz and Louis Jeantet foundations, the Swiss National Research Fund, the National Pole of Research (NCCR) 'Frontiers in Genetics' and the European community (EUMORPHIA). J.C. was supported by an NRSA from the National Institutes of Health (USA).

Supplementary material

Supplementary material for this article is available at
http://dev.biologists.org/cgi/content/full/132/13/3055/DC1

References

Brazma, A., Parkinson, H., Sarkans, U., Shojatalab, M., Vilo, J., Abeygunawardena, N., Holloway, E., Kapushesky, M., Kemmeren, P., Lara, G. G. et al. (2003). ArrayExpress–a public repository for microarray gene expression data at the EBI. *Nucleic Acids Res.* **31**, 68-71.

Bruhl, T., Urbich, C., Aicher, D., Acker-Palmer, A., Zeiher, A. M. and Dimmeler, S. (2004). Homeobox A9 transcriptionally regulates the EphB4 receptor to modulate endothelial cell migration and tube formation. *Circ. Res.* **94**, 743-751.

Brunet, A., Park, J., Tran, H., Hu, L. S., Hemmings, B. A. and Greenberg,

M. E. (2001). Protein kinase SGK mediates survival signals by phosphorylating the forkhead transcription factor FKHRL1 (FOXO3a). *Mol. Cell. Biol.* **21**, 952-965.

Buj-Bello, A., Adu, J., Pinon, L. G., Horton, A., Thompson, J., Rosenthal, A., Chinchetru, M., Buchman, V. L. and Davies, A. M. (1997). Neurturin responsiveness requires a GPI-linked receptor and the Ret receptor tyrosine kinase. *Nature* **387**, 721-724.

Chen, J. and Ruley, H. E. (1998). An enhancer element in the *EphA2 (Eck)* gene sufficient for rhombomere-specific expression is activated by HOXA1 and HOXB1 homeobox proteins. *J. Biol. Chem.* **273**, 24670-24675.

Chen, Y. and Zhao, X. (1998). Shaping limbs by apoptosis. *J. Exp. Zool.* **282**, 691-702.

Compagni, A., Logan, M., Klein, R. and Adams, R. H. (2003). Control of skeletal patterning by ephrinB1-EphB interactions. *Dev. Cell* **5**, 217-230.

Davis, A. P., Witte, D. P., Hsieh-Li, H. M., Potter, S. S. and Capecchi, M. R. (1995). Absence of radius and ulna in mice lacking *hoxa-11* and *hoxd-11*. *Nature* **375**, 791-795.

Dolle, P., Izpisua-Belmonte, J. C., Brown, J. M., Tickle, C. and Duboule, D. (1991). *HOX-4* genes and the morphogenesis of mammalian genitalia. *Genes Dev.* **5**, 1767-1777.

Dolle, P., Dierich, A., LeMeur, M., Schimmang, T., Schuhbaur, B., Chambon, P. and Duboule, D. (1993). Disruption of the *Hoxd-13* gene induces localized heterochrony leading to mice with neotenic limbs. *Cell* **75**, 431-441.

Duboule, D. and Wilkins, A. S. (1998). The evolution of 'bricolage'. *Trends Genet.* **14**, 54-59.

Fromental-Ramain, C., Warot, X., Messadecq, N., LeMeur, M., Dolle, P. and Chambon, P. (1996). *Hoxa-13* and *Hoxd-13* play a crucial role in the patterning of the limb autopod. *Development* **122**, 2997-3011.

Gebelein, B., McKay, D. J. and Mann, R. S. (2004). Direct integration of Hox and segmentation gene inputs during *Drosophila* development. *Nature* **431**, 653-659.

Goodman, F. R. (2002). Limb malformations and the human HOX genes. *Am. J. Med. Genet.* **112**, 256-265.

Haraguchi, R., Suzuki, K., Murakami, R., Sakai, M., Kamikawa, M., Kengaku, M., Sekine, K., Kawano, H., Kato, S., Ueno, N. et al. (2000). Molecular analysis of external genitalia formation: the role of fibroblast growth factor (*Fgf*) genes during genital tubercle formation. *Development* **127**, 2471-2479.

Haraguchi, R., Mo, R., Hui, C., Motoyama, J., Makino, S., Shiroishi, T., Gaffield, W. and Yamada, G. (2001). Unique functions of *Sonic hedgehog* signaling during external genitalia development. *Development* **128**, 4241-4250.

Hedlund, E., Karsten, S. L., Kudo, L., Geschwind, D. H. and Carpenter, E. M. (2004). Identification of a *Hoxd10*-regulated transcriptional network and combinatorial interactions with *Hoxa10* during spinal cord development. *J. Neurosci. Res.* **75**, 307-319.

Hertweck, M., Gobel, C. and Baumeister, R. (2004). *C. elegans* SGK-1 is the critical component in the Akt/PKB kinase complex to control stress response and life span. *Dev. Cell* **6**, 577-588.

Hiltunen, P. H. and Airaksinen, M. S. (2004). Sympathetic cholinergic target innervation requires GDNF family receptor GFR alpha 2. *Mol. Cell Neurosci.* **26**, 450-457.

Hubbell, E., Liu, W. M. and Mei, R. (2002). Robust estimators for expression analysis. *Bioinformatics* **18**, 1585-1592.

Kawakami, Y., Rodriguez-Leon, J., Koth, C. M., Buscher, D., Itoh, T., Raya, A., Ng, J. K., Esteban, C. R., Takahashi, S., Henrique, D. et al. (2003). MKP3 mediates the cellular response to *FGF8* signalling in the vertebrate limb. *Nat. Cell Biol.* **5**, 513-519.

Klein, R. D., Sherman, D., Ho, W. H., Stone, D., Bennett, G. L., Moffat, B., Vandlen, R., Simmons, L., Gu, Q., Hongo, J. A. et al. (1997). A GPI-linked protein that interacts with Ret to form a candidate neurturin receptor. *Nature* **387**, 717-721.

Knosp, W. M., Scott, V., Bachinger, H. P. and Stadler, H. S. (2004). HOXA13 regulates the expression of bone morphogenetic proteins 2 and 7 to control distal limb morphogenesis. *Development* **131**, 4581-4592.

Kondo, T., Zakany, J., Innis, J. W. and Duboule, D. (1997). Of fingers, toes and penises. *Nature* **390**, 29.

Lang, F. and Cohen, P. (2001). Regulation and physiological roles of serum- and glucocorticoid-induced protein kinase isoforms. *Sci. STKE* **108**, RE17.

Laurikainen, A., Hiltunen, J. O., Thomas-Crusells, J., Vanhatalo, S., Arumae, U., Airaksinen, M. S., Klinge, E. and Saarma, M. (2000). Neurturin is a neurotrophic factor for penile parasympathetic neurons in adult rat. *J. Neurobiol.* **43**, 198-205.

Lavrovsky, Y., Song, C. S., Chatterjee, B. and Roy, A. K. (1998). A rapid and reliable PCR-based assay for gene transmission and sex determination in newborn transgenic mice. *Transgenic Res.* **7**, 319-320.

Lee, E., Lein, E. S. and Firestone, G. L. (2001). Tissue-specific expression of the transcriptionally regulated serum and glucocorticoid-inducible protein kinase (Sgk) during mouse embryogenesis. *Mech. Dev.* **103**, 177-181.

Leussink, B., Brouwer, A., el Khattabi, M., Poelmann, R. E., Gittenberger-de Groot, A. C. and Meijlink, F. (1995). Expression patterns of the paired-related homeobox genes *MHox/Prx1* and *S8/Prx2* suggest roles in development of the heart and the forebrain. *Mech. Dev.* **52**, 51-64.

Li, C. and Hung Wong, W. (2001). Model-based analysis of oligonucleotide arrays: model validation, design issues and standard error application. *Genome Biol.* **2**, RESEARCH0032.

Liu, W. M., Mei, R., Di X., Ryder, T. B., Hubbell, E., Dee, S., Webster, T. A., Harrington, C. A., Ho, M. H., Baid, J. et al. (2002). Analysis of high density expression microarrays with signed-rank call algorithms. *Bioinformatics* **18**, 1593-1599.

Mann, R. S. and Affolter, M. (1998). Hox proteins meet more partners. *Curr. Opin. Genet. Dev.* **8**, 423-429.

Mercader, N., Leonardo, E., Azpiazu, N., Serrano, A., Morata, G., Martinez, C. and Torres, M. (1999). Conserved regulation of proximodistal limb axis development by Meis1/Hth. *Nature* **402**, 425-429.

Mikosz, C. A., Brickley, D. R., Sharkey, M. S., Moran, T. W. and Conzen, S. D. (2001). Glucocorticoid receptor-mediated protection from apoptosis is associated with induction of the serine/threonine survival kinase gene, *sgk-1*. *J. Biol. Chem.* **276**, 16649-16654.

Morgan, E. A., Nguyen, S. B., Scott, V. and Stadler, H. S. (2003). Loss of *Bmp7* and *Fgf8* signaling in Hoxa13-mutant mice causes hypospadia. *Development* **130**, 3095-3109.

Niederreither, K., Vermot, J., Schuhbaur, B., Chambon, P. and Dolle, P. (2002). Embryonic retinoic acid synthesis is required for forelimb growth and anteroposterior patterning in the mouse. *Development* **129**, 3563-3574.

Peirson, S. N., Butler, J. N. and Foster, R. G. (2003). Experimental validation of novel and conventional approaches to quantitative real-time PCR data analysis. *Nucleic Acids Res.* **31**, e73.

Peng, X. D., Xu, P. Z., Chen, M. L., Hahn-Windgassen, A., Skeen, J., Jacobs, J., Sundararajan, D., Chen, W. S., Crawford, S. E., Coleman, K. G. et al. (2003). Dwarfism, impaired skin development, skeletal muscle atrophy, delayed bone development, and impeded adipogenesis in mice lacking Akt1 and Akt2. *Genes Dev.* **17**, 1352-1365.

Perriton, C. L., Powles, N., Chiang, C., Maconochie, M. K. and Cohn, M. J. (2002). *Sonic hedgehog* signaling from the urethral epithelium controls external genital development. *Dev. Biol.* **247**, 26-46.

Phelan, M. L. and Featherstone, M. S. (1997). Distinct HOX N-terminal arm residues are responsible for specificity of DNA recognition by HOX monomers and HOX.PBX heterodimers. *J. Biol. Chem.* **272**, 8635-8643.

Poliakov, A., Cotrina, M. and Wilkinson, D. G. (2004). Diverse roles of eph receptors and ephrins in the regulation of cell migration and tissue assembly. *Dev. Cell* **7**, 465-480.

Popperl, H. and Featherstone, M. S. (1992). An autoregulatory element of the murine *Hox-4.2* gene. *EMBO J.* **11**, 3673-3680.

Popperl, H., Bienz, M., Studer, M., Chan, S. K., Aparicio, S., Brenner, S., Mann, R. S. and Krumlauf, R. (1995). Segmental expression of *Hoxb-1* is controlled by a highly conserved autoregulatory loop dependent upon exd/pbx. *Cell* **81**, 1031-1042.

Post, L. C. and Innis, J. W. (1999). Altered Hox expression and increased cell death distinguish Hypodactyly from *Hoxa13* null mice. *Int. J. Dev. Biol.* **43**, 287-294.

Pruett, N. D., Tkatchenko, T. V., Jave-Suarez, L., Jacobs, D. F., Potter, C. S., Tkatchenko, A. V., Schweizer, J. and Awgulewitsch, A. (2004). Krtap16, characterization of a new hair keratin-associated protein (KAP) gene complex on mouse chromosome 16 and evidence for regulation by *Hoxc13*. *J. Biol. Chem.* **279**, 51524-51533.

Riddle, R. D., Johnson, R. L., Laufer, E. and Tabin, C. (1993). *Sonic hedgehog* mediates the polarizing activity of the ZPA. *Cell* **75**, 1401-1416.

Ririe, K. M., Rasmussen, R. P. and Wittwer, C. T. (1997). Product differentiation by analysis of DNA melting curves during the polymerase chain reaction. *Anal. Biochem.* **245**, 154-160.

Rossi, J., Luukko, K., Poteryaev, D., Laurikainen, A., Sun, Y. F., Laakso, T., Eerikainen, S., Tuominen, R., Lakso, M., Rauvala, H. et al. (1999). Retarded growth and deficits in the enteric and parasympathetic nervous system in mice lacking GFR alpha2, a functional neurturin receptor. *Neuron* **22**, 243-252.

Satokata, I., Ma, L., Ohshima, H., Bei, M., Woo, I., Nishizawa, K., Maeda,

T., Takano, Y., Uchiyama, M., Heaney, S. et al. (2000). Msx2 deficiency in mice causes pleiotropic defects in bone growth and ectodermal organ formation. *Nat. Genet.* **24**, 391-395.

Shen, W. F., Montgomery, J. C., Rozenfeld, S., Moskow, J. J., Lawrence, H. J., Buchberg, A. M. and Largman, C. (1997). AbdB-like Hox proteins stabilize DNA binding by the Meis1 homeodomain proteins. *Mol. Cell. Biol.* **17**, 6448-6458.

Spitz, F., Gonzalez, F., Peichel, C., Vogt, T. F., Duboule, D. and Zakany, J. (2001). Large scale transgenic and cluster deletion analysis of the HoxD complex separate an ancestral regulatory module from evolutionary innovations. *Genes Dev.* **15**, 2209-2214.

Stadler, H. S., Higgins, K. M. and Capecchi, M. R. (2001). Loss of *Eph-receptor* expression correlates with loss of cell adhesion and chondrogenic capacity in *Hoxa13* mutant limbs. *Development* **128**, 4177-4188.

Sugino, H., Hamada, S., Yasuda, R., Tuji, A., Matsuda, Y., Fujita, M. and Yagi, T. (2000). Genomic organization of the family of CNR cadherin genes in mice and humans. *Genomics* **63**, 75-87.

Sun, X., Mariani, F. V. and Martin, G. R. (2002). Functions of FGF signalling from the apical ectodermal ridge in limb development. *Nature* **418**, 501-508.

Suzuki, K., Ogino, Y., Murakami, R., Satoh, Y., Bachiller, D. and Yamada, G. (2002). Embryonic development of mouse external genitalia: insights into a unique mode of organogenesis. *Evol. Dev.* **4**, 133-141.

Suzuki, K., Bachiller, D., Chen, Y. P., Kamikawa, M., Ogi, H., Haraguchi, R., Ogino, Y., Minami, Y., Mishina, Y., Ahn, K. et al. (2003). Regulation of outgrowth and apoptosis for the terminal appendage: external genitalia development by concerted actions of BMP signaling. *Development* **130**, 6209-6220.

Tickle, C. (2003). Patterning systems – from one end of the limb to the other. *Dev. Cell* **4**, 449-458.

Vaidya, A., Pniak, A., Lemke, G. and Brown, A. (2003). *EphA3* null mutants do not demonstrate motor axon guidance defects. *Mol. Cell. Biol.* **23**, 8092-8098.

Valerius, M. T., Patterson, L. T., Feng, Y. and Potter, S. S. (2002). Hoxa 11 is upstream of Integrin alpha8 expression in the developing kidney. *Proc. Natl. Acad. Sci. USA* **99**, 8090-8095.

van der Hoeven, F., Zakany, J. and Duboule, D. (1996). Gene transpositions in the *HoxD* complex reveal a hierarchy of regulatory controls. *Cell* **85**, 1025-1035.

Vandesompele, J., De Preter, K., Pattyn, F., Poppe, B., Van Roy, N., De Paepe, A. and Speleman, F. (2002). Accurate normalization of real-time quantitative RT-PCR data by geometric averaging of multiple internal control genes. *Genome Biol.* **3**, RESEARCH0034.

Wada, N., Tanaka, H., Ide, H. and Nohno, T. (2003). *Ephrin-A2* regulates position-specific cell affinity and is involved in cartilage morphogenesis in the chick limb bud. *Dev. Biol.* **264**, 550-563.

Warot, X., Fromental-Ramain, C., Fraulob, V., Chambon, P. and Dolle, P. (1997). Gene dosage-dependent effects of the *Hoxa-13* and *Hoxd-13* mutations on morphogenesis of the terminal parts of the digestive and urogenital tracts. *Development* **124**, 4781-4791.

Wu, Z., Irizarry, R. A., Gentleman, R., Murillo, F. M. and Spencer, F. (2004). A model based background adjustment for oligonucleotide expression arrays. *J. Am. Stat. Assoc.* **99**, 909-917.

Wulff, P., Vallon, V., Huang, D. Y., Volkl, H., Yu, F., Richter, K., Jansen, M., Schlunz, M., Klingel, K., Loffing, J. et al. (2002). Impaired renal Na(+) retention in the sgk1-knockout mouse. *J. Clin. Invest.* **110**, 1263-1268.

Zakany, J. and Duboule, D. (1996). Synpolydactyly in mice with a targeted deficiency in the *HoxD* complex. *Nature* **384**, 69-71.

Zakany, J., Fromental-Ramain, C., Warot, X. and Duboule, D. (1997). Regulation of number and size of digits by posterior Hox genes: a dose-dependent mechanism with potential evolutionary implications. *Proc. Natl. Acad. Sci. USA* **94**, 13695-13700.

Zakany, J., Kmita, M. and Duboule, D. (2004). A dual role for Hox genes in limb anterior-posterior asymmetry. *Science* **304**, 1669-1672.

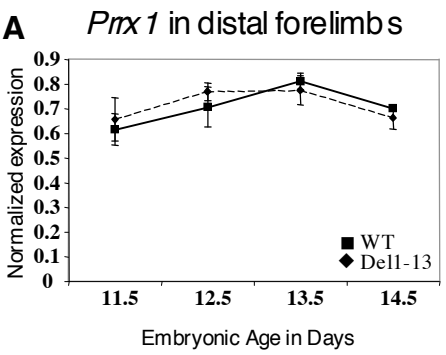
A
Prrx1 in distal forelimbs
Normalized expression
0.9
0.8
0.7
0.6
0.5
0.4
0.3
0.2
0.1
0
WT
Del1-13
11.5
12.5
13.5
14.5
Embryonic Age in Days

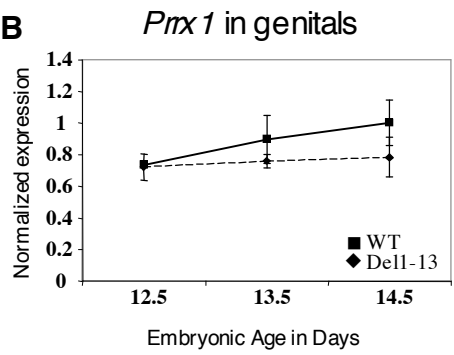
B
Prrx1 in genitals
Normalized expression
1.4
1.2
1
0.8
0.6
0.4
0.2
0
WT
Del1-13
12.5
13.5
14.5
Embryonic Age in Days

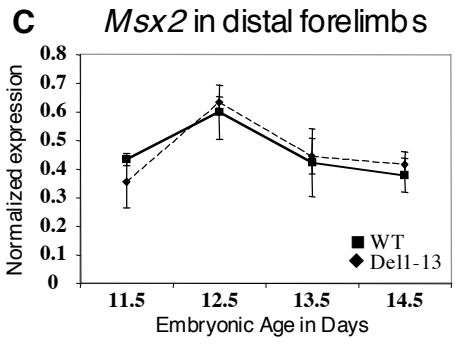
C
Msx2 in distal forelimbs
Normalized expression
0.8
0.7
0.6
0.5
0.4
0.3
0.2
0.1
0
WT
Del1-13
11.5
12.5
13.5
14.5
Embryonic Age in Days

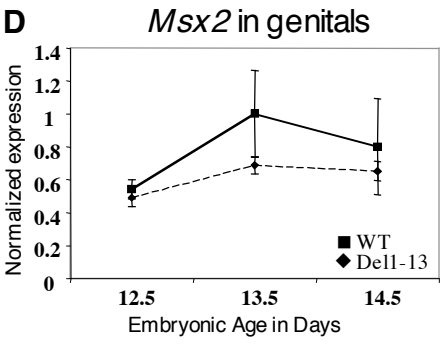
D
Msx2 in genitals
Normalized expression
1.4
1.2
1
0.8
0.6
0.4
0.2
0
WT
Del1-13
12.5
13.5
14.5
Embryonic Age in Days

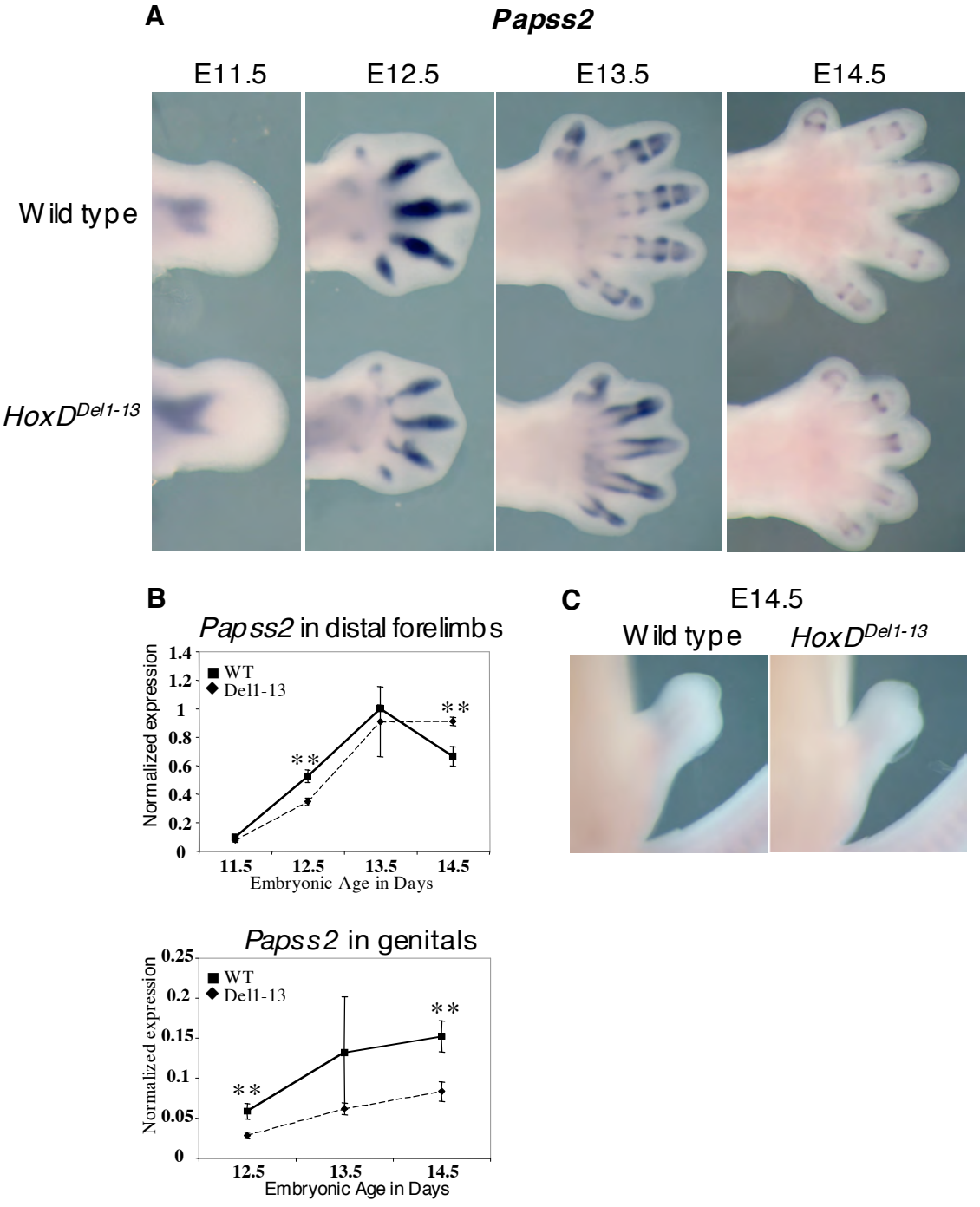
A
Papss2
E11.5
E12.5
E13.5
E14.5
Wild type
HoxD Del1-13
B
Papss2 in distal forelimbs
Normalized expression
WT
Del1-13
**
**
11.5
12.5
13.5
14.5
Embryonic Age in Days
Papss2 in genitals
Normalized expression
WT
Del1-13
**
**
12.5
13.5
14.5
Embryonic Age in Days
C
E14.5
Wild type
HoxD Del1-13

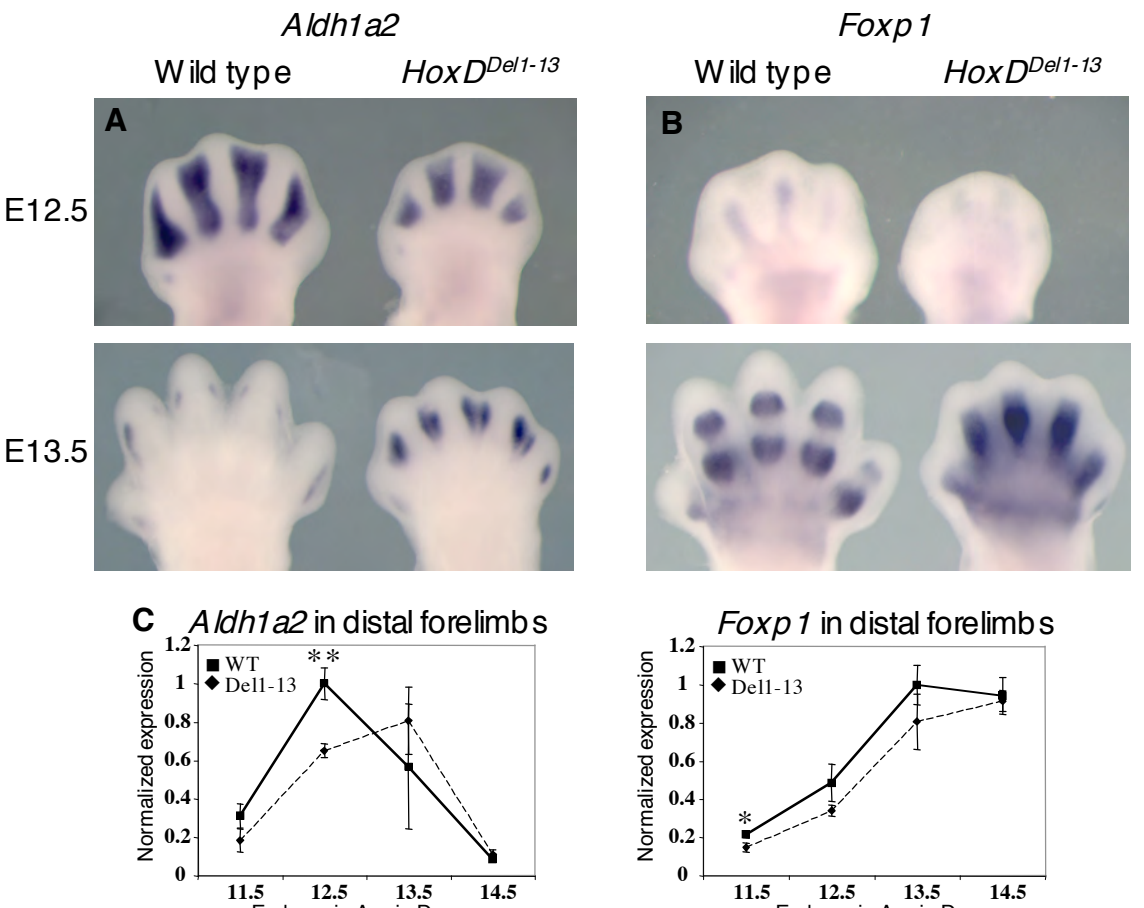
Aldh1a2
Wild type
HoxD Del1-13
Foxp1
Wild type
HoxD Del1-13
A
B
E12.5
E13.5
C
Aldh1a2 in distal forelimbs
Foxp1 in distal forelimbs
WT
Del1-13
Normalized expression
Embryonic Age in Days
11.5
12.5
13.5
14.5
0
0.2
0.4
0.6
0.8
1
1.2
**
*

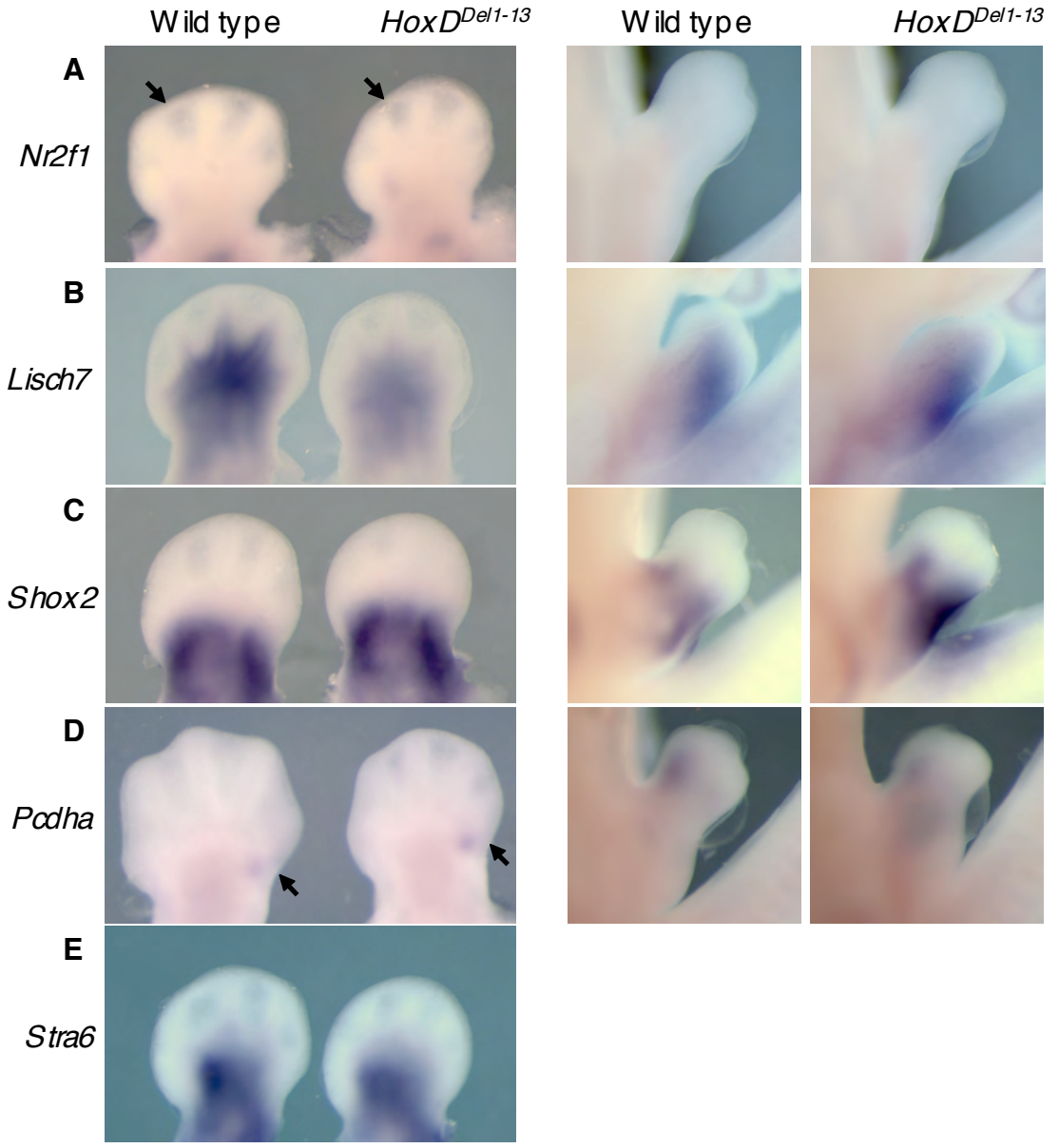
Wild type
HoxD^Del1-13
Wild type
HoxD^Del1-13
A
Nr2f1
B
Lisch7
C
Shox2
D
Pcdha
E
Stra6